



1

2

3

4

Heterogeneous uptake of amines onto kaolinite in the temperature range of 232-300 K

5

6

Y. Liu^{1,2,3}, Y. Ge^{1,3}, H. He^{1,2,3*}

7

1. State Key Joint Laboratory of Environment Simulation and Pollution

8

Control, Research Center for Eco-Environmental Sciences, Chinese Academy

9

of Sciences, Beijing, 100085, China

10

2. Center for Excellence in Urban Atmospheric Environment, Institute of Urban

11

Environment, Chinese Academy of Sciences, Xiamen 361021, China.

12

3. University of Chinese Academy of Sciences, Beijing, 100049, China

13

* Correspondence to: H. He (honghe@rcees.ac.cn)

14 **Abstract:**

15 Amines contribute to atmospheric reactive nitrogen (N_r) deposition, new particle
16 formation and the growth of nano- and sub-micron particles. Heterogeneous uptake of
17 amines by ammonium compounds and organic aerosols has been recognized as an
18 important source of particulate organic nitrogen. However, the role of mineral dust in
19 the chemical cycle of amines is unknown because the corresponding reaction kinetics
20 are unavailable. In this study, the heterogeneous uptake of methylamine (MA),
21 dimethylamine (DMA) and trimethylamine (TMA) by kaolinite was investigated in the
22 temperature range of 232-300 K using a Knudsen cell reactor. Lewis acid sites on
23 kaolinite were identified as dominant contributors to the uptake of amines, utilizing
24 Fourier transform infrared spectroscopy. The uptake coefficients (γ) were derived from
25 the mass accommodation coefficients based on the temperature dependence of the γ .
26 The initial effective uptake coefficients (γ_{eff}) were $(2.27 \pm 0.26) \times 10^{-3}$, $(1.71 \pm 0.26) \times 10^{-3}$
27 and $(2.95 \pm 0.63) \times 10^{-3}$, respectively, for MA, DMA and TMA on kaolinite at 300 K,
28 while they increased ~3-fold with decreasing temperature from 300 K to 232 K. The
29 adsorption enthalpies (ΔH_{obs}) of MA, DMA and TMA on kaolinite were -7.8 ± 0.8 , -9.9
30 ± 2.9 and -9.4 ± 1.0 kJ mol⁻¹, respectively, and the corresponding entropy values (ΔS_{obs})
31 were -77.1 ± 3.2 , -84.1 ± 1.8 and -80.6 ± 3.7 J K⁻¹ mol⁻¹. The lifetimes of MA, DMA and
32 TMA attributable to heterogeneous uptake by mineral dust were estimated to be 7.2,
33 11.5 and 7.7 h, respectively. These values were comparable to the lifetimes of amines
34 consumed by OH oxidation. Our results reveal that uptake by mineral dust should be
35 considered in models simulating the chemical cycle of amines in the atmosphere. The
36 results will also aid in understanding the possible impacts of amines on human health,
37 air quality, and climate effects.

38



39 1.0 Introduction

40 Over the past 200 years, atmospheric emissions of nitrogen-containing compounds
41 have increased significantly due to increased anthropological emissions from intensive
42 fossil-fuel combustion, agricultural activity and animal husbandry (Keene et al., 2002).
43 This has amplified atmospheric reactive nitrogen (N_r) concentrations and increased
44 atmospheric N_r deposition rates (Meunier et al., 2016). These elevated N_r fluxes may
45 significantly perturb terrestrial, aquatic, estuarine and coastal marine ecosystems (Liu
46 et al., 2013; van Breemen, 2002). However, reliable predictive capabilities for the
47 impacts of N_r on ecosystem require the accurate quantification of the deposition fluxes
48 (Keene et al., 2002) as well as the transformation of atmospheric N_r . Amines, whose
49 atmospheric concentrations are typically 1–14 nmol N m⁻³ and 1–2 orders of magnitude
50 lower than that of ammonia (Ge et al., 2011; Qiu and Zhang, 2013), are emitted into the
51 atmosphere from marine organisms, animal husbandry, biomass burning, sewage
52 treatment, meat cooking, automobiles and industrial processes (Zhang et al., 2012).
53 Compared with inorganic nitrogen, the budget and the atmospheric chemistry of organic
54 nitrogen, including amines, are still poorly characterized (Keene et al., 2002; Cornell et
55 al., 2003).

56 Amines may contribute 10–20% of the organic content of ambient particles, and
57 over one hundred different amine species have been frequently observed in the particle
58 phase (Qiu and Zhang, 2013). It has been recognized that acid-base reactions between
59 amines and nitric acid (Murphy et al., 2007), sulfuric acid (Almeida et al., 2013; Jen et
60 al., 2014; Bzdek et al., 2011; Wang et al., 2010a), and methanesulfonic acid (MSA)
61 (Nishino et al., 2014) contribute to nucleation (Smith et al., 2010; Almeida et al., 2013),
62 and growth of nano- and sub-micron particles (Qiu and Zhang, 2013). Heterogeneous
63 uptake of amines onto (NH₄)₂SO₄ (Bzdek et al., 2010a; Qiu et al., 2011; Chan and Chan,



64 2012), NH_4HSO_4 (Qiu et al., 2011;Liu et al., 2012a;Chan and Chan, 2012), NH_4NO_3
65 (Liu et al., 2012a;Chan and Chan, 2012;Lloyd et al., 2009), NH_4Cl (Liu et al.,
66 2012a;Chan and Chan, 2012), humic acid, and citric acid (Liu et al., 2012b) has been
67 proposed as another possible explanation for particulate amines observed in ambient
68 particles. The uptake coefficient (γ) of amines on ultra-fine nanometer-scale ammonium
69 particles is close to unity (Bzdek et al., 2010b), whereas it is on the order of $\sim 10^{-3}$ - 10^{-2}
70 on coarse particles (Qiu et al., 2011;Liu et al., 2012a) and fine particles of 20-500 nm
71 particle diameter (Lloyd et al., 2009). The γ of amines on citric acid and humic acid is
72 on the order of $\sim 10^{-3}$ and $\sim 10^{-5}$ (Liu et al., 2012b), respectively. Similar to the reaction
73 between NH_3 and secondary organic aerosol (SOA) (Liu et al., 2015b;Nguyen et al.,
74 2013;Lee et al., 2013b) or between $(\text{NH}_4)_2\text{SO}_4$ and glyoxal (Galloway et al.,
75 2009;Trainic et al., 2011;Yu et al., 2011;Lee et al., 2013a), carbonyl groups in organic
76 aerosol can also take up primary and secondary amines to form imine and enamine
77 compounds in both bulk solution and the particle phase (Zarzana et al., 2012;De Haan
78 et al., 2009). This may explain the high-MW constituents with a large fraction of
79 carbon–nitrogen bonds observed in ambient particles (Wang et al., 2010b).

80 Mineral dust, with a global source strength of 1000-3000 Tg year⁻¹, is one of the
81 most important contributors to atmospheric particles and plays an important role as a
82 reactive surface in the global troposphere (Dentener et al., 1996). The reactive uptake
83 of SO_2 , HNO_3 , NO_2 , N_2O_5 , O_3 and HO_2 on mineral dust has been widely investigated
84 (Usher et al., 2003) and has been found to significantly influence sulfate (Zheng et al.,
85 2015), nitrate and O_3 formation by affecting trace gas concentrations and the
86 tropospheric oxidation capacity through surface processes (Zhang and Carmichael,
87 1999). On the other hand, the temperature in the atmosphere varies with latitude,
88 longitude, and altitude above the Earth's surface, as well as with season and time of day.



89 For example, the tropospheric temperature for latitude 40 °N during June decreases from
90 room temperature (r.t.) to 220 K with an increase in altitude. The temperature at the
91 tropopause can reach values much lower than 220 K: down to 180 K above the Antarctic
92 in winter (Smith, 2003). For most atmospheric reactions, the reaction kinetics is
93 sensitive to temperature. Thus, it is very important to measure the reaction kinetics
94 (Crowley et al., 2010; Atkinson et al., 2006) and its temperature dependence for trace
95 gases, including amines, (Qiu and Zhang, 2013) on mineral dust in order to fully
96 understand the relevant atmospheric chemistry. However, at the present time, the role
97 of mineral dust in the chemical cycle of amines in the atmosphere is unknown, because
98 the corresponding temperature-dependent reaction kinetics for these reactions is
99 unavailable.

100 In this work, heterogeneous uptake of amines including methylamine (MA),
101 dimethylamine (DMA) and trimethylamine (TMA) by kaolinite, which has been found
102 to be a typical mineral dust crystalline phase in atmospheric particles, was investigated
103 in the temperature range of 232-300 K. The temperature dependence of uptake
104 coefficients, relevant thermodynamic parameters and associated environmental
105 implications are discussed. The results of this study will aid in understanding the
106 atmospheric chemistry of amines.

107

108 **2.0 EXPERIMENTAL DETAILS**

109 **2.1 Uptake experiments.** Uptake of amines was investigated using a Knudsen cell
110 reactor coupled to a mass spectrometer (KCMS). This system has been described in
111 detail elsewhere (Liu et al., 2012b; Liu et al., 2012a; Liu et al., 2010a; Liu and He,
112 2009 ; Liu et al., 2008 ; Liu et al., 2008). Briefly, the KCMS was composed of three
113 stages with different working pressures. The first one was the Knudsen cell reactor



114 working at $\sim 10^{-4}$ Torr. It consisted of a stainless steel chamber with a gas inlet controlled
115 by a leak valve, an escape aperture whose area was adjustable using an iris diaphragm,
116 a sample holder attached to the top surface of a circulating fluid bath, and an ion gauge
117 (BOC Edwards). The sample in the sample holder could be exposed to or isolated from
118 the reactants by a lid connected to a linear translator. The temperature of the sample
119 holder was controlled using a thermostat and cryofluid pump (DFY-5/80, Henan Yuhua
120 laboratory instrument Co, Ltd.) and measured with an embedded Pt resistance
121 thermometer. The second stage was a transition chamber pumped by a $60 \text{ L}\cdot\text{s}^{-1}$
122 turbomolecular pump (BOC Edwards). The working pressure in this stage was $\sim 10^{-7}$
123 Torr and monitored with an ion gauge (BOC Edwards). In the third stage, a quadrupole
124 mass spectrometer (QMS, Hiden HAL 3F PIC) was housed in a vacuum chamber
125 pumped by a $300 \text{ L}\cdot\text{s}^{-1}$ turbomolecular pump (Pfeiffer) at a working pressure of $\sim 10^{-9}$
126 Torr measured using an ion gauge (BOC Edwards).

127 Kaolinite powder was dispersed evenly on the Teflon sample holder with ethanol,
128 heated at 373 K for 2 h after the solvent was evaporated at room temperature, and then
129 out-gassed at 298 K in the Knudsen cell reactor for 8 h to reach a base pressure of
130 approximately 5.0×10^{-7} Torr. Amine (MA, DMA or TMA) equilibrated with the
131 corresponding aqueous solution was introduced into the reactor chamber through the
132 leak valve. The pressure of amines in the reactor was kept at $3.5 \pm 0.2 \times 10^{-5}$ Torr to
133 ensure free molecular flow in the reactor. The reactor chamber was passivated with
134 amines while the sample was isolated from the reactant gas by the sample cover, until
135 a steady state QMS signal was established. Then, the sample was exposed to the amines
136 for uptake experiments.

137 The observed uptake coefficients (γ_{obs}) were calculated with a Knudsen cell
138 equation (Tabor et al., 1994; Ullerstam et al. 2003; Underwood et al., 2000), namely,



$$\gamma_{obs} = \frac{A_h}{A_g} \cdot \frac{I_0 - I}{I} \quad (1)$$

139 where A_h is the effective area of the escape aperture (0.88 mm²) during uptake
140 experiments and measured according to methods reported previously (Liu et al., 2009a,
141 b and 2010a, b); A_g is the geometric area of the sample holder (326 mm²); and I_0 and I
142 are the mass spectral intensities with the sample holder closed and open, respectively.
143 The reaction kinetics were measured in the temperature range of 232-300 K.
144

145 Analytical grade MA (40 % in H₂O, Alfa Aesar), DMA (40 % in H₂O, Aladdin
146 Chemistry Co. Ltd) and TMA (28 % in H₂O, TCI), ethanol (Sinopharm Chemical
147 Reagent Co. Ltd) and kaolinite (Aladdin Chemistry Co. Ltd) were used as received. The
148 specific surface area (N₂-BET) of kaolinite was 71 m² g⁻¹, measured using a
149 Quantachrome Autosorb-1-C instrument.

150 **2.2 *In situ* infrared spectra measurements.** The surface species during uptake of
151 amine by kaolinite were monitored using *in situ* attenuated total reflection Fourier
152 transform infrared spectroscopy (ATR-FTIR). The particles were prepared by
153 depositing small droplets containing kaolinite suspension onto the ATR crystal (ZnSe)
154 with an atomizer, followed by purging with 1 L·min⁻¹ zero air to obtain dry particles in
155 the ATR chamber. After the particles were dried, which was monitored by observing
156 the IR bands of water, amine vapor was introduced into the reactor by a flow of 200
157 mL·min⁻¹ zero air through a water bubbler containing the amine. *In situ* IR spectra were
158 recorded on a Nicolet 6700 (Thermo Nicolet Instrument Corporation, USA) Fourier
159 transform infrared (FTIR) spectrometer equipped with an *in situ* attenuated total
160 reflection chamber and a high sensitivity mercury cadmium telluride (MCT) detector
161 cooled by liquid N₂. The IR spectra were recorded taking the dried kaolinite as reference
162 during uptake of amine. All spectra reported here were recorded at a resolution of 4 cm⁻¹
163 for 100 scans.



164 **3.0 Results and Discussion**

165 **3.1 Uptake of amines on kaolinite at 300 K.** Figure 1A, B and C show the typical
166 uptake profiles for MA, DMA and TMA, respectively. Figure 1D, E and F show the
167 corresponding profiles of the observed uptake coefficients, which will be discussed later.
168 In these experiments, the sample mass was ~20 mg and the temperature was held at 300
169 K. The partial pressures of amines in the reactor were around 5.0×10^{-5} Torr, which
170 corresponded to ~60 ppbv of amines in the atmosphere. Both the molecular ion peak
171 and the largest fragment, i.e. m/z 31 and 30 for MA, m/z 45 and 44 for DMA, and m/z
172 59 and 58 for the TMA, were scanned to verify that the species were being correctly
173 measured. As shown in Fig. 1A-C, the relative signals of the two monitored mass
174 channels for each amine coincided very well. The normalized QMS signals decreased
175 significantly when the kaolinite samples were exposed to amines. The lowest values of
176 the normalized QMS signal (I/I_0) were 0.45, 0.63, and 0.47 for MA, DMA and TMA on
177 kaolinite, respectively, under this specific condition. Then, the I/I_0 increased gradually
178 with exposure time due to the surface saturation of amines. The uptake behaviors for
179 these amines on kaolinite were similar to those on humic acid as observed in our
180 previous work (Liu et al., 2012b), whereas they were different from the uptake
181 behaviors of amines on ammonium compounds (Liu et al., 2012a). The recoveries of
182 the uptake curves of amines can be explained by the saturation of the surface reactive
183 sites on kaolinite. However, exchange reactions take place between amines and
184 ammonium compounds, resulting in ammonia as the product (Liu et al., 2012a; Qiu et
185 al., 2011; Bzdek et al., 2010a); subsequently, a continuous uptake of amines
186 accompanied by ammonia formation was observed within a certain period of time (Liu
187 et al., 2012a).

188 Kaolinite is a 1:1 layer mineral. Each layer of the mineral consists of an alumina



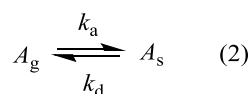
189 octahedral sheet and a silica tetrahedral sheet that share a common plane of oxygen
190 atoms (Brindley and Robinson, 1945) and repeating layers of the mineral are hydrogen-
191 bonded together (Miranda-Trevino¹ and Coles, 2003). Usually, both Lewis acid and
192 Brønsted acid sites are present on metal oxides (Busca, 1999; Benvenuti et al., 1992).
193 Pyridine, piperidine or *n*-butylamine have been widely used as probe molecules to
194 measure the type of acid site and the acidity of metal oxide materials (Busca, 1999). To
195 confirm the reactive sites on kaolinite, infrared spectra were collected using an *in situ*
196 ATR-FTIR.

197 Figure 2 shows the ATR-FTIR spectra of MA, DMA and TMA adsorbed on
198 kaolinite for 30 min at 300 K. It should be pointed out that the absolute intensities for
199 the bands of surface species resulting from adsorption of different amines were not
200 identical, even for the adsorbed water bands at ~ 3400 and ~ 1640 cm^{-1} . This might be
201 related to different mass loading of kaolinite deposited on the ZnSe crystal via
202 atomization. Therefore, we only qualitatively discuss the assignments of the related
203 surface species. The typical IR bands of amines, such as the $\nu_{\text{as}}(\text{CH}_3)$ and $\nu_{\text{s}}(\text{CH}_3)$ bands
204 at 2962 and 2860 cm^{-1} accompanied by the $\delta(\text{CH}_3)$ bands at ~ 1400 cm^{-1} and the $\rho(\text{CH}_3)$
205 bands from 985 cm^{-1} to 1290 cm^{-1} (Murphy et al., 1993), the overtone/combination
206 bands of $-\text{CH}_3$ and CN groups in the range of 2300 - 2700 cm^{-1} (Murphy et al., 1993),
207 the $\nu_{\text{s}}(\text{CN})$ bands at ~ 1260 and 850 cm^{-1} (Durgaprasad et al., 1971), $\delta(\text{NH}_2)$ of MA at
208 1606 cm^{-1} (Nunes et al., 2005) and the $\delta(\text{NH})$ band (NIST) and/or $\delta(\text{CH}_3)$ of DMA at
209 1473 cm^{-1} (Lin et al., 2014) in Fig. 2, confirmed the adsorption of amines on kaolinite.
210 In a previous work, the IR bands at 1484 and 984 cm^{-1} were assigned to the
211 characteristic bands of protonated TMA ($(\text{CH}_3)_3\text{NH}^+$) in an acidic solution mixed with
212 TMA and on the surface of polyethylene (PE) treated by TMA (Ongwandee et al., 2007).
213 In this work, two bands at 1477 - 1467 cm^{-1} and 971 cm^{-1} were observed, as shown in



214 Fig. 2, and were probably related to the protonated amines (MAH⁺, DMAH⁺ and
 215 TMAH⁺). In particular, a strong peak at 1473 cm⁻¹ was observed (Fig. 2B), while the
 216 band was very weak for the spectra in Fig. 2A and C. However, this band was very
 217 close to the δ(NH) band at ~1470 cm⁻¹ in DMA (NIST database) and/or δ(CH₃) (Lin et
 218 al., 2014) in amines. On the other hand, it should be noted that formation of protonated
 219 amines requires surface OH (Brønsted acid). However, as shown in Fig. 2, the surface
 220 hydroxyl (-OH) in the range of 3600-3750 cm⁻¹ (Miranda-Trevino¹ and Coles, 2003)
 221 was not consumed when the kaolinite was exposed to MA, DMA or TMA. This
 222 indicates that the content of reactive Brønsted acid sites on the kaolinite must be very
 223 low even if the bands at 1477-1467 cm⁻¹ originated from the protonated amines.
 224 Therefore, Lewis acid sites on the kaolinite predominantly contributed to the uptake of
 225 amines as observed in Figs. 1 and 2 in this study. This was similar to the adsorption of
 226 DMA and N,N-dimethyl formamide (DMF) on TiO₂, for which Lewis acid sites were
 227 identified as the reactive sites (Lin et al., 2014).

228 As shown in Fig. 1, the saturation times for the amines on kaolinite varied slightly
 229 depending upon the number of substituted methyl groups in the amines. For example,
 230 the saturation time was ~20 min for MA, while it decreased to ~15 min and ~10 min
 231 for DMA and TMA, respectively. This implies a different rate of increase for the surface
 232 coverage among the different amines during adsorption. According to the gas-particle
 233 equilibrium of amines on the surface of kaolinite as shown in Eq. (2),



234

235 the surface concentration of amines on kaolinite can be described as,

$$\frac{dc_{A,s}}{dt} = k_a c_{A,g} - k_d c_{A,s} \quad (3)$$

236

237 where k_a and k_d are the adsorption coefficient and desorption coefficient, respectively;



238 $c_{A,g}$ and $c_{A,s}$ are the concentration of amines in the gas phase and on the surface,
239 respectively. When replacing $c_{A,s}$ with the surface coverage of amine ($\theta=c_{A,s}/c_T$), the
240 time dependent surface coverage of amine is

$$241 \quad \frac{d\theta}{dt} = \frac{k_a c_{A,g}}{c_T} - k_d \theta \quad (4)$$

242 or,

$$243 \quad \theta = \frac{k_a c_{A,g}}{k_d c_T} - \frac{1}{k_d} \exp(-k_d t) \quad (5)$$

244 where c_T is the total reactive or adsorptive sites or the saturated adsorption capacity for
245 amines on kaolinite; t is the exposure time. Therefore, the saturation time of amines on
246 kaolinite depends on the adsorption coefficient, the desorption coefficient, the total
247 number of reactive sites and the concentration of amines in the gas phase. If all the
248 layers of the packed kaolinite particles are assumed to be available to amine molecules,
249 the saturated adsorption capacity of MA, DMA and TMA on kaolinite is estimated to
250 be 1.7×10^{19} , 7.3×10^{18} and 5.7×10^{18} molecules mg^{-1} , respectively, under this reaction
251 condition. These values will be lower if amines cannot penetrate all the layers in the
252 sample holder. This will be discussed later. The adsorption capacities are inversely
253 correlated with the cross-sectional area of MA (0.243 nm^2), DMA (0.323 nm^2), and
254 TMA (0.394 nm^2) (Liu et al., 2012b). This means that a part of the Lewis acid sites
255 accessible to MA on the kaolinite surface would not be accessible to amines with larger
256 molecular volume or cross-sectional area.

257 **3.2 Reaction kinetics of amines on kaolinite at 300 K.** Based on the measured QMS
258 signals of amines as shown in Fig. 1, the uptake coefficients were calculated using Eq.
259 (1). Figure 1D, E and F show the evolution of γ_{obs} of MA, DMA and TMA, respectively,
260 as a function of exposure time on kaolinite at 300 K. The initial γ_{obs} varied from
261 $\sim 2.0 \times 10^{-3}$ to $\sim 3.0 \times 10^{-3}$ for these amines at 300 K, while the γ_{obs} decreased markedly



262 with increasing exposure time as shown in Fig. 1. This is in agreement with the results
263 observed for most of the reactive gases, such as NO₃, N₂O₅ (Tang et al., 2010), NO₂
264 (Wang et al., 2012;Ndour et al., 2008;Liu et al., 2015a), O₃ (Hanisch and Crowley,
265 2003), HONO (El Zein and Bedjanian, 2012) and COS (Liu et al., 2010a) on typical
266 atmospheric particles because of surface saturation, as discussed above.

267 For packed powder samples in a sample holder, diffusion of reactive molecules into
268 the underlying layers was widely observed in previous works (Liu et al., 2010b;Liu et
269 al., 2010a;Keyser et al., 1991;Underwood et al., 2001;Grassian, 2002). Therefore, the
270 effective uptake coefficient (γ_{eff}) might be overestimated when calculating the γ with
271 Eq. (1) in which the geometric area of the sample holder instead of the effective surface
272 area is considered. The KML model (Keyser et al., 1991), LMD model (Underwood et
273 al., 2001;Grassian, 2002) and FPL model (Hoffman et al., 2003) have been developed
274 to estimate the effective surface area of uptake for heterogeneous reactions. The linear
275 mass dependent (LMD) model (Underwood et al., 2001), which was developed based
276 on the KML model, has been widely used for data interpretation in Knudsen cell
277 experiments. That is,

$$278 \quad \gamma_{\text{obs}} = \gamma_{\text{eff}} m_{\text{eff}} S_{\text{BET}} / A_{\text{g}} \quad (6)$$

279 or,

$$280 \quad \gamma_{\text{eff}} = A_{\text{g}} \text{Slope} / S_{\text{BET}} \quad (7)$$

281 where γ_{eff} is the effective uptake coefficient; m_{eff} is the effective sample mass; S_{BET} is
282 the specific surface area of the sample; A_{g} is the geometric area of the sample holder;
283 *Slope* is the slope of the plot of γ_{obs} versus sample mass in the linear regime (mg^{-1}).
284 Thus, γ_{eff} can be determined by measuring the m_{eff} of reactive molecules or the slope of
285 the γ_{obs} versus sample mass for multilayer powder samples when the powder samples
286 evenly cover the sample holder.



287 Figure 3 shows the γ_{obs} of the three amines on kaolinite in the mass range of 20-
288 100 mg at 300 K. When the sample mass was less than 20 mg, the sample holder could
289 not be evenly covered by particles. In such a case, γ_{obs} would be underestimated with
290 Eq. (1). Therefore, uptake experiments with sample mass below 20 mg were not
291 performed. However, as shown in Fig. 3, the γ_{obs} of MA, DMA and TMA were
292 independent of the sample mass of kaolinite within experimental uncertainty. This is
293 similar to the uptake of amines on $(\text{NH}_4)_2\text{SO}_4$, NH_4HSO_4 , NH_4NO_3 , and NH_4Cl (Qiu et
294 al., 2011; Liu et al., 2012a) and citric acid (Liu et al., 2012b), the uptake of HNO_3 on
295 soot (Muñoz and Rossi, 2002) and N_2O_5 and H_2O on mineral dust (Seisel et al.,
296 2005; Seisel et al., 2004). This indicates that the underlying layers of the kaolinite
297 sample contributed very little to amine uptake.

298 The probe depth of a reactive gas in a packed powder sample can be expressed by
299 using a factor for the effect of gas-phase diffusion into the underlying layers (Keyser et
300 al., 1991; Underwood et al., 2001).

$$301 \quad \eta = \frac{1}{\phi} \tanh(\phi) \quad (8)$$

$$302 \quad \phi = \frac{m}{\rho_b A_g d_p} \left(\frac{3\rho_b}{\rho_t - \rho_b} \right) \left(\frac{3\tau\gamma_{eff}}{4} \right)^{1/2} \quad (9)$$

303 Thus,

$$304 \quad \gamma_{obs} = \gamma_{eff} (A_e + \eta A_i) / A_g \quad (10)$$

305 where η is a factor to account for the effect of gas-phase diffusion into the underlying
306 layers ($0 \leq \eta \leq 1$); m is the sample mass; ρ_b and ρ_t are the bulk density and the true density
307 of the sample, respectively; d_p is the particle diameter of the sample; τ is the tortuosity
308 factor of the sample; A_g is the geometric area of the sample holder; A_e and A_i are the
309 area of the first layer of the sample (external) and the area of the underlying layers of
310 the sample (internal), respectively. The reactive gas can effectively diffuse into the



311 underlying layers if η is close to 1, while the contribution of the underlying layers to
312 the reactive gas uptake is negligible when η is close to 0. Therefore, a large γ_{eff} should
313 result in a small η or small probe depth, and vice versa. This means that the γ_{eff} of
314 amines on kaolinite should be close to or equal to the γ_{obs} in this study. Thus, the mean
315 γ_{obs} measured at different sample mass were taken as the corresponding γ_{eff} of amines
316 on kaolinite and summarized in Table 1. They were $(2.27 \pm 0.26) \times 10^{-3}$, $(1.71 \pm 0.26) \times 10^{-3}$
317 and $(2.95 \pm 0.63) \times 10^{-3}$, respectively, for MA, DMA and TMA on kaolinite at 300 K.
318 The γ_{eff} of amines on kaolinite were on the same order as the γ_{eff} of amines on coarse
319 particles, including $(\text{NH}_4)_2\text{SO}_4$, NH_4NO_3 , NH_4Cl and citric acid (Liu et al., 2012a; Liu
320 et al., 2012b) investigated in our previous work, and on 20-500 nm NH_4NO_3 particles
321 (Lloyd et al., 2009), while they were 1 and 3 orders of magnitude lower than that on the
322 surface of a H_2SO_4 solution (Wang et al., 2010a) and ammonium salt clusters (Bzdek et
323 al., 2010b), respectively.

324 There are several factors affecting the heterogeneous reaction kinetics of amines
325 with the typical components of atmospheric particles. First, particle size plays an
326 important role in the reactivity of amines. For example, the first-order γ of DMA on 1-
327 2 nm $[(\text{NH}_4)_3(\text{SO}_4)_2]^+$ clusters was close to unity (Bzdek et al., 2010b), while γ
328 decreased to 10^{-3} - 10^{-2} on coarse particles of $(\text{NH}_4)_2\text{SO}_4$ (Liu et al., 2012a; Qiu et al.,
329 2011). Second, strong acidity of a particle or solution favors the reactions between
330 amines and the substrates. The γ of amines on citric acid, with a pK_{a1} of 3.1, were 2
331 orders of magnitude higher than those on humic acid, with a pK_{a1} of 5 (Liu et al., 2012b).
332 H_2SO_4 solution with higher H_2SO_4 content also showed a slightly larger γ for amines
333 (Wang et al., 2010a). Even for different ammonium compounds, the H with stronger
334 acidity in the NH_4 group showed a higher reactivity toward MA (Liu et al., 2012a).
335 Third, the steric effect of amines has an effect on the reactivity on the same substrate.



336 It has been found that the γ of amines on citric acid and humic acid linearly decreased
337 with the cross-sectional area of the amines (Liu et al., 2012b). Finally, reaction
338 conditions such as temperature and humidity should have an influence on the reactivity
339 between amines and particles. Wang et al. (Wang et al., 2010a) observed that the γ of
340 amines negatively depended on temperature due to the negative temperature
341 dependence of the mass accommodation coefficient. This might partially explain the
342 difference in the measured γ of MA on $(\text{NH}_4)_2\text{SO}_4$ between our previous work (Liu et
343 al., 2012a) and Qiu's work (Qiu et al., 2011). Chan et al. (Chan and Chan, 2012) found
344 that a high RH favored the formation of TEAH sulfate in the displacement reaction
345 between TEA and $(\text{NH}_4)_2\text{SO}_4$. Under the same reaction conditions, the properties of
346 both the particles and the amines should have an effect on the heterogeneous reactivity
347 of amines.

348 Figure 4A shows a box chart of the measured γ_{eff} of these three amines on kaolinite
349 at 300 K. Means comparisons were performed with the Dunn-Sidak method. ANOVA
350 analysis demonstrated a statistically significant difference in the mean γ_{eff} among MA,
351 DMA and TMA at the 0.05 level ($F=49.3$, $P=2.54\times 10^{-13}$). The γ_{eff} of MA was
352 significantly larger than that of DMA, while it was significantly smaller than that of
353 TMA. This should be ascribed to the difference in the properties of the amines, because
354 the influence of the particle size and acidity on the reactivity, as mentioned above, can
355 be ruled out when the same substrate is used. The reactivity sequence observed in this
356 study is in contrast with that between amines and organic acids (Liu et al., 2012b). This
357 might be explained by the different types of reactive sites for organic acids and kaolinite
358 toward amines. For organic acids, the $-\text{COOH}$ group is the reactive site (Liu et al.,
359 2012b), while Lewis acid sites predominantly contribute to the uptake of amines on
360 kaolinite in this study, as discussed in Section 3.1. The interaction between $-\text{COOH}$ and



361 amines should be more sensitive to the neighboring groups than that between M^+ (Lewis
362 acid) and amines, because the C-C bonds in organic acid are more flexible than the M-
363 O (metal-oxygen) bonds in kaolinite. This means that the steric effect of amines is
364 unimportant for the reaction between amines and kaolinite. As shown in Fig. 4B, the
365 γ_{eff} of amines on kaolinite are positively correlated with the basicity of amines (H. K.
366 Hall, 1957). Therefore, the slightly higher reactivity of TMA on kaolinite can be
367 explained by its strong basicity and the lower reactivity of DMA on kaolinite should be
368 related to its weak basicity.

369 **3.3 Temperature dependence of amine uptake on kaolinite.** Table 2 summarizes the
370 mean γ_{eff} at different temperature. The γ_{eff} were in the range of $(2.27 \pm 0.26) \times 10^{-3}$ -
371 $(5.79 \pm 0.64) \times 10^{-3}$ for MA, $(1.71 \pm 0.26) \times 10^{-3}$ - $(6.04 \pm 1.24) \times 10^{-3}$ for DMA and
372 $(2.95 \pm 0.63) \times 10^{-3}$ - $(9.24 \pm 0.26) \times 10^{-3}$ for TMA. For all three amines, the γ_{eff} increased
373 with decreasing temperature. This is similar to the uptake of amines on the surface of
374 H_2SO_4 solution (Wang et al., 2010a), the uptake of HNO_3 , HCl and N_2O_5 on the surface
375 of water droplets (Doren et al., 1999) and the uptake of N_2O_5 on the surface of
376 $(NH_4)_2SO_4$ (Griffiths and Anthony Cox, 2009).

377 Uptake of amines on kaolinite is the result of the coupled processes of mass
378 accommodation (gas-to-particle transfer) and reaction with the reactive sites (mainly
379 Lewis acid) on the surface of kaolinite. Thus,

$$380 \quad \frac{1}{\gamma} = \frac{1}{\alpha} + \frac{1}{\Gamma_{rxn}} \quad (11)$$

381 where α is the mass accommodation coefficient; Γ_{rxn} is the surface reaction resistance
382 (Ammann et al., 2003). If the reaction on the surface is fast enough, accommodation at
383 the surface of amines becomes the rate determining step (RDS) and γ is equal to α .
384 According to the thermodynamic model of mass accommodation (Davidovits et al.,
385 2006), the relationship between the α and temperature can be described as,



$$\ln \frac{\alpha}{1-\alpha} = \ln \frac{\gamma}{1-\gamma} = \frac{-\Delta H_{obs}}{RT} + \frac{\Delta S_{obs}}{R} \quad (12)$$

where R is the ideal gas constant; T is reaction temperature. Therefore, the adsorption enthalpy (ΔH_{obs}) and entropy (ΔS_{obs}) for amines on kaolinite can be obtained by equation (12) (Liu et al., 2010b; Hudson et al., 2002; Davidovits et al., 2006). Figure 5 shows the plot of $\gamma/(1-\gamma)$ versus inverse temperature. The temperature dependence of the γ of amines on kaolinite is consistent with accommodation-controlled uptake with the assumption $\gamma=\alpha$. This also satisfactorily explained the independence of the observed uptake coefficient on sample mass as discussed in Section 3.2, because of the large γ .

The ΔH_{obs} and ΔS_{obs} for adsorption of MA on kaolinite were determined to be $-7.8 \pm 0.8 \text{ kJ mol}^{-1}$ and $-77.1 \pm 3.2 \text{ J K}^{-1} \text{ mol}^{-1}$, respectively. They were $-9.9 \pm 2.9 \text{ kJ mol}^{-1}$ and $-84.1 \pm 11.8 \text{ J K}^{-1} \text{ mol}^{-1}$ for DMA and $-9.4 \pm 1.0 \text{ kJ mol}^{-1}$ and $-80.6 \pm 3.7 \text{ J K}^{-1} \text{ mol}^{-1}$ for TMA. The ΔH_{obs} or ΔS_{obs} values are not significantly different at the 0.05 level among the different amines. The ΔH_{obs} for uptake of amines on kaolinite are comparable with that of carbonyl sulfide ($-10.7 \pm 1.1 \text{ kJ mol}^{-1}$) on kaolinite (Liu et al., 2010b), while they are smaller than the ΔH_{obs} of N_2O_5 on $(\text{NH}_4)_2\text{SO}_4$ (-33 kJ mol^{-1}) (Griffiths and Anthony Cox, 2009) and N_2O_5 on sulfuric acid aerosol (-25 kJ mol^{-1}) (Hallquist et al., 2000). The relative small ΔH_{obs} values of amines on kaolinite demonstrate that amines weakly adsorb on kaolinite.

The empirical formulas relating γ_t of amines on kaolinite and temperature are given as

$$\gamma_{eff}(\text{MA}) = \frac{\exp(938.8/T-9.3)}{1+\exp(938.8/T-9.3)} \quad (13)$$

$$\gamma_{eff}(\text{DMA}) = \frac{\exp(1193.8/T-10.1)}{1+\exp(1193.8/T-9.3)} \quad (14)$$

$$\gamma_{eff}(\text{TMA}) = \frac{\exp(1126.5/T-9.6)}{1+\exp(1126.5/T-9.6)} \quad (15)$$

Thus, the γ_t at other temperatures can be obtained using these equations.



410 **4 Conclusions and environmental implications**

411 The uptake of amines on kaolinite was investigated within a temperature range of 232-
412 300 K. It was found that Lewis acid sites on kaolinite were the main contributors to the
413 uptake of amines. The initial effective uptake coefficients of amines were
414 $(2.27 \pm 0.26) \times 10^{-3}$, $(1.71 \pm 0.26) \times 10^{-3}$ and $(2.95 \pm 0.63) \times 10^{-3}$, respectively, for MA, DMA
415 and TMA on kaolinite at 300 K. The basicity of amines was weakly correlated with the
416 reactivity at 300 K, namely, TMA, with the strongest basicity, showed the highest
417 reactivity on kaolinite, and vice versa for DMA. The uptake coefficients increased ~3-
418 fold with decreasing temperature from 300 K to 232 K. Based on the temperature
419 dependence of the uptake coefficients, the uptake of amines was predominantly
420 ascribed to mass accommodation. The ΔH_{obs} of MA, DMA and TMA on kaolinite were
421 -7.8 ± 0.8 , -9.9 ± 2.9 and -9.4 ± 1.0 kJ mol⁻¹, respectively. The corresponding ΔS_{obs} were
422 -77.1 ± 3.2 , -84.1 ± 11.8 and -80.6 ± 3.7 J K⁻¹ mol⁻¹. The empirical formula relating γ and
423 temperature can be expressed as shown in Eqs. (13)-(15).

424 With the measured uptake coefficients, the lifetimes of amines attributable to
425 uptake by kaolinite can be estimated by

$$426 \quad \tau = \frac{4}{\gamma_{\text{eff}} \bar{v} SA} \quad (16)$$

427 where \bar{v} is the average velocity of amines (m s⁻¹); γ_{eff} is the effective uptake
428 coefficient at 300 K; and SA is the surface area of particles in the dust event (m² m⁻³).
429 If we assume that all mineral dust is in the form of kaolinite, and the dust loading is 150
430 $\mu\text{m}^2 \text{cm}^{-3}$ (de Reus et al., 2000; Frinak et al., 2004) under extreme conditions, the
431 lifetimes of MA, DMA and TMA due to heterogeneous uptake onto dust were estimated
432 to be 7.2, 11.5 and 7.7 h, respectively. In the atmosphere, oxidation by OH was
433 considered to be the main degradation pathway of amines. The second-order rate
434 constants of aliphatic amines toward OH are $(2-6) \times 10^{-11}$ cm³ molecule⁻¹ s⁻¹ (Atkinson,



435 1986). Thus, their lifetimes are in the range of 4.6-13.8 h with the assumption of a 24 h
436 average OH concentration of 1.0×10^6 molecules cm^{-3} (Prinn et al., 2001). Therefore,
437 the estimated lifetimes of amines related to heterogeneous uptake by mineral dust are
438 comparable to those consumed by OH oxidation. Of course, the contribution of
439 heterogeneous uptake to the amine sink might be overestimated here, because the
440 uptake coefficient decreased with exposure time quickly as shown in Fig. 1. It should
441 be noted that the γ_t values of amines on kaolinite increased significantly at low
442 temperature as shown in Table 2. On the other hand, high concentrations of mineral
443 dust are possible near particular emission sources, such as agriculture, which is an
444 important source of amines (Kuhn et al., 2011). Therefore, mineral dust may have an
445 important influence on the local concentration of amines, especially in low temperature
446 regions with high concentrations of mineral dust. Finally, uptake experiments were
447 performed in a Knudsen cell reactor in this study. Although water vapor was also
448 introduced into the reactor along with amines, the RH was still lower than 1 %. If high
449 RH can also promote the uptake of amines on mineral dust as observed on $(\text{NH}_4)_2\text{SO}_4$,
450 NH_4NO_3 and NH_4Cl (Chan and Chan, 2012), the contribution of mineral dust to the
451 amine sink will be enhanced.

452 Recent studies have found that alkylammonium sulfates with lower vapor pressure
453 than that of ammonium sulfate are more thermally stable than their counterparts (Lavi
454 et al., 2013) and the displacement reactions of alkylamines with ammonium sulfate lead
455 to a transition from the crystalline to an amorphous phase, improved water uptake (Qiu
456 and Zhang, 2012) and CCN activity (Lavi et al., 2013), and less scattering ability for
457 360 and 420 nm radiation (Lavi et al., 2013). This means that heterogeneous reactions
458 greatly modify the properties of aerosols (Gomez-Hernandez et al., 2016). Kaolinite
459 particles have been confirmed as effective ice nuclei (IN) (Wex et al., 2014; Salam et al.,



460 2006), while physically adsorbed amines on kaolinite can reduce the water wettability
461 of kaolinite (Kitahara and Williamson, 1964). This means that heterogeneous uptake of
462 amines on kaolinite may have an influence on the IN ability of kaolinite, although this
463 needs to be confirmed with experiments in the future.

464 Alkylammonium sulfate salts, even in freshly nucleated nanoparticles (lower than 10
465 nm in diameter), will not be likely to undergo particle to gas partitioning at room
466 temperature because of their thermal stability and ultralow vapor pressures (Lavi et al.,
467 2013). However, physical adsorption with small enthalpy takes place between amines
468 and kaolinite. This means that adsorbed amines probably at or near the emission sources
469 of amines can be transported with dust to other regions, and subsequently might
470 undergo particle-to-gas partitioning in air with a lower concentration of amines, and
471 subsequently, further participate in new particle formation with acids or displacement
472 reactions with ammonium compounds. In this process, mineral dust takes on the role of
473 a carrier or reservoir of amines.

474

475 **Acknowledgements**

476 This research was financially supported by the National Natural Science Foundation of
477 China (41275131) and the Strategic Priority Research Program of Chinese Academy of
478 Sciences (XDB05040100, XDB05010300).

479

480 **References:**

481 Almeida, J., Schobesberger, S., Kurten, A., Ortega, I. K., Kupiainen-Maatta, O., Praplan, A. P., Adamov,
482 A., Amorim, A., Bianchi, F., Breitenlechner, M., David, A., Dommen, J., Donahue, N. M., Downard, A.,
483 Dunne, E., Duplissy, J., Ehrhart, S., Flagan, R. C., Franchin, A., Guida, R., Hakala, J., Hansel, A.,
484 Heinritzi, M., Henschel, H., Jokinen, T., Junninen, H., Kajos, M., Kangasluoma, J., Keskinen, H., Kupc,
485 A., Kurten, T., Kvashin, A. N., Laaksonen, A., Lehtipalo, K., Leiminger, M., Leppa, J., Loukonen, V.,
486 Makhmutov, V., Mathot, S., McGrath, M. J., Nieminen, T., Olenius, T., Onnela, A., Petaja, T., Riccobono,
487 F., Riipinen, I., Rissanen, M., Rondo, L., Ruuskanen, T., Santos, F. D., Sarnela, N., Schallhart, S.,
488 Schnitzhofer, R., Seinfeld, J. H., Simon, M., Sipila, M., Stozhkov, Y., Stratmann, F., Tome, A., Trostl, J.,
489 Tsagkogeorgas, G., Vaattovaara, P., Viisanen, Y., Virtanen, A., Vrtala, A., Wagner, P. E., Weingartner, E.,
490 Wex, H., Williamson, C., Wimmer, D., Ye, P., Yli-Juuti, T., Carslaw, K. S., Kulmala, M., Curtius, J.,



- 491 Baltensperger, U., Worsnop, D. R., Vehkamäki, H., and Kirkby, J.: Molecular understanding of sulphuric
492 acid-amine particle nucleation in the atmosphere, *Nature*, 502, 359-363, doi: 10.1038/nature12663, 2013.
493 Ammann, M., Poschl, U., and Rudich, Y.: Effects of reversible adsorption and Langmuir-Hinshelwood
494 surface reactions on gas uptake by atmospheric particles, *Phys. Chem. Chem. Phys.*, 5, 351-356, doi:
495 10.1039/B208708A, 2003.
- 496 Atkinson, R.: Kinetics and Mechanisms of the Gas-Phase Reactions of the Hydroxyl Radical with
497 Organic Compounds under Atmospheric Conditions, *Chem. Rev.*, 85, 69-201, doi: 10.1021/cr00071a004,
498 1986.
- 499 Atkinson, R., Baulch, D. L., Cox, R. A., Crowley, J. N., Hampson, R. F., Hynes, R. G., Jenkin, M. E.,
500 Rossi, M. J., Troe, J., and Subcommittee, I.: Evaluated kinetic and photochemical data for atmospheric
501 chemistry: Volume II - gas phase reactions of organic species, *Atmos. Chem. Phys.*, 6, 3625-4055,
502 doi:10.5194/acp-6-3625-2006, 2006.
- 503 Benvenuti, E. V., Gushikem, Y., and Davanzo, C. U.: Pyridine used as a probe for internal bronsted acid
504 sites in pyrochlore antimony(v) oxide - an infrared-spectroscopy study, *Appl. Spectrosc.*, 46, 1474-1476,
505 doi: 10.1366/000370292789619179, 1992.
- 506 Brindley, G. W., and Robinson, K.: Structure of Kaolinite, *Nature*, 156, 661-662, doi:10.1038/156661b0,
507 1945.
- 508 Busca, G.: The surface acidity of solid oxides and its characterization by IR spectroscopic methods. An
509 attempt at systematization, *Phys. Chem. Chem. Phys.*, 1, 723-736, doi: 10.1039/A808366E, 1999.
- 510 Bzdek, B. R., Ridge, D. P., and Johnston, M. V.: Size-Dependent Reactions of Ammonium Bisulfate
511 Clusters with Dimethylamine, *J. Phys. Chem. A*, 114, 11638-11644, doi: 10.1021/jp106363m, 2010a.
- 512 Bzdek, B. R., Ridge, D. P., and Johnston, M. V.: Amine exchange into ammonium bisulfate and
513 ammonium nitrate nuclei, *Atmos. Chem. Phys.*, 10, 3495-3503, doi: 10.5194/acp-10-3495-2010, 2010b.
- 514 Bzdek, B. R., Ridge, D. P., and Johnston, M. V.: Amine reactivity with charged sulfuric acid clusters,
515 *Atmos. Chem. Phys.*, 11, 8735-8743, doi:10.5194/acp-11-8735-2011, 2011.
- 516 Chan, L. P., and Chan, C. K.: Displacement of Ammonium from Aerosol Particles by Uptake of
517 Triethylamine, *Aerosol Sci. Technol.*, 46, 236-247, doi: 10.1080/02786826.2011.618815, 2012.
- 518 Cornell, S. E., Jickells, T. D., Cape, J. N., Rowland, A. P., and Duce, R. A.: Organic nitrogen deposition
519 on land and coastal environments: a review of methods and data, *Atmos. Environ.*, 37, 2173-2191, doi:
520 10.1016/S1352-2310(03)00133-X, 2003.
- 521 Crowley, J. N., Ammann, M., Cox, R. A., Hynes, R. G., Jenkin, M. E., Mellouki, A., Rossi, M. J., Troe,
522 J., and Wallington, T. J.: Evaluated kinetic and photochemical data for atmospheric chemistry: Volume
523 V – heterogeneous reactions on solid substrates, *Atmos. Chem. Phys.*, 10, 9059-9223, doi: 10.5194/acp-
524 10-9059-2010, 2010.
- 525 Davidovits, P., Kolb, C. E., Williams, L. R., Jayne, J. T., and Worsnop, D. R.: Mass accommodation and
526 chemical reactions at gas-liquid interfaces, *Chem. Rev.*, 106, 1323-1354, doi: 10.1021/cr040366k, 2006.
- 527 De Haan, D. O., Tolbert, M. A., and Jimenez, J. L.: Atmospheric condensed-phase reactions of glyoxal
528 with methylamine, *Geophys. Res. Lett.*, 36, L11819, doi: 10.1029/2009gl037441, 2009.
- 529 Dentener, F. J., Carmichael, G. R., Zhang, Y., Lelieveld, J., and Crutzen, P. J.: Role of mineral aerosol as
530 a reactive surface in the global troposphere, *J. Geophys. Res.*, 101, 22869-22889, doi:
531 10.1029/96JD01818, 1996.
- 532 Doren, J. M. V., Watson, L. R., Davidovits, P., Worsnop, D. R., Zahniser, M. S., and Kolb, C. E.:
533 Temperature dependence of the uptake coefficients of nitric acid, hydrochloric acid and nitrogen oxide
534 (N₂O₅) by water droplets, *J. Phys. Chem.*, 39, 3265-3269, doi: 10.1021/j100371a009, 1999.
- 535 Durgaprasad, G., Sathyanarayana, D. N., and Patel, C. C.: Infrared Spectra and Normal Vibrations of
536 N,N-Dimethylformamide and N,N-Dimethylthioformamide, *Bull. Chem. Soc. Jpn.*, 44, 316-322, doi:
537 10.1246/bcsj.44.316, 1971.
- 538 El Zein, A., and Bedjanian, Y.: Reactive Uptake of HONO to TiO₂ Surface: “Dark” Reaction, *J. Phys.*
539 *Chem. A*, 116, 3665-3672, doi: 10.1021/jp300859w, 2012.
- 540 Galloway, M. M., Chhabra, P. S., Chan, A. W. H., Surratt, J. D., Flagan, R. C., Seinfeld, J. H., and Keutsch,
541 F. N.: Glyoxal uptake on ammonium sulphate seed aerosol: reaction products and reversibility of uptake
542 under dark and irradiated conditions, *Atmos. Chem. Phys.*, 9, 3331-3345, doi: 10.5194/acp-9-3331-2009,
543 2009.
- 544 Ge, X., Wexler, A. S., and Clegg, S. L.: Atmospheric amines - Part I. A review, *Atmos. Environ.*, 45, 524-
545 546, doi: 10.1016/j.atmosenv.2010.10.012, 2011.
- 546 Gomez-Hernandez, M., McKeown, M., Secret, J., Marrero-Ortiz, W., Lavi, A., Rudich, Y., Collins, D.
547 R., and Zhang, R.: Hygroscopic Characteristics of Alkylammonium Carboxylate Aerosols, *Environ. Sci.*
548 *Technol.*, 50, 2292-2300, doi: 10.1021/acs.est.5b04691, 2016.
- 549 Grassian, V. H.: Chemical Reactions of Nitrogen Oxides on the Surface of Oxide, Carbonate, Soot, and
550 Mineral Dust Particles: Implications for the Chemical Balance of the Troposphere, *J. Phys. Chem. A*,



- 551 106, 860-877, doi: 10.1021/jp012139h, 2002.
- 552 Griffiths, P. T., and Anthony Cox, R.: Temperature dependence of heterogeneous uptake of N₂O₅ by
 553 ammonium sulfate aerosol, *Atmos. Sci. Lett.*, 10, 159-163, doi: 10.1002/asl.225, 2009.
- 554 H. K. Hall, J.: Correlation of the Base Strengths of Amines, *J. Am. Chem. Soc.*, 79, 5441-5444, doi:
 555 10.1021/ja01577a030, 1957.
- 556 Hallquist, M., Stewart, D. J., Jacob Baker, A., and Cox, R. A.: Hydrolysis of N₂O₅ on Submicron
 557 Sulfuric Acid Aerosols, *J. Phys. Chem. A*, 104, 3984-3990, doi: 10.1021/jp9939625, 2000.
- 558 Hanisch, F., and Crowley, J. N.: Ozone decomposition on Saharan dust: an experimental investigation,
 559 *Atmos. Chem. Phys.*, 3, 119-130, doi: 10.5194/acp-3-119-2003, 2003.
- 560 Hoffman, R. C., Kaleuati, M. A., and Finlayson-Pitts, B. J.: Knudsen Cell Studies of the Reaction of
 561 Gaseous HNO₃ with NaCl Using Less than a Single Layer of Particles at 298 K: A Modified Mechanism,
 562 *J. Phys. Chem. A.*, 107, 7818-7826, doi: 10.1021/jp030611o, 2003.
- 563 Hudson, P. K., Shilling, J. E., Tolbert, M. A., and Toon, O. B.: Uptake of Nitric Acid on Ice at
 564 Tropospheric Temperatures: Implications for Cirrus Clouds, *J. Phys. Chem. A.*, 106, 9874-9882, doi:
 565 10.1021/jp020508j, 2002.
- 566 Jen, C. N., McMurry, P. H., and Hanson, D. R.: Stabilization of sulfuric acid dimers by ammonia,
 567 methylamine, dimethylamine, and trimethylamine, *J. Geophys. Res.- Atmos.*, 119, 2014JD021592, doi:
 568 10.1002/2014JD021592, 2014.
- 569 Keene, W. C., Montag, J. A., Maben, J. R., Southwell, M., Leonard, J., Church, T. M., Moody, J. L., and
 570 Galloway, J. N.: Organic nitrogen in precipitation over Eastern North America, *Atmos. Environ.*, 36,
 571 4529-4540, doi: 10.1016/S1352-2310(02)00403-X, 2002.
- 572 Keyser, L. F., Moore, S. B., and Leu, M. T.: Surface reaction and pore diffusion in flow-tube reactors, *J.*
 573 *Phys. Chem.*, 95, 5496-5502, doi: 10.1021/j100167a026, 1991.
- 574 Kitahara, A., and Williamson, W. O.: Wettability of kaolinite treated with ammonia, methylamine,
 575 ethylamine, or their corresponding cations, *J. Am. Ceram. Soc.*, 47, 313-317, doi: 10.1111/j.1151-
 576 2916.1964.tb12991.x, 1964.
- 577 Kuhn, U., Sintermann, J., Spirig, C., Jocher, M., Ammann, C., and Neftel, A.: Basic biogenic aerosol
 578 precursors: Agricultural source attribution of volatile amines revised, *Geophys. Res. Lett.*, 38, L16811,
 579 doi: 10.1029/2011gl047958, 2011.
- 580 Lavi, A., Bluvshstein, N., Segre, E., Segev, L., Flores, M., and Rudich, Y.: Thermochemical, Cloud
 581 Condensation Nucleation Ability, and Optical Properties of Alkyl Aminium Sulfate Aerosols, *J. Phys.*
 582 *Chem. C*, 117, 22412-22421, doi: 10.1021/jp403180s, 2013.
- 583 Lee, A. K. Y., Zhao, R., Li, R., Liggio, J., Li, S.-M., and Abbatt, J. P. D.: Formation of Light Absorbing
 584 Organo-Nitrogen Species from Evaporation of Droplets Containing Glyoxal and Ammonium Sulfate,
 585 *Environ. Sci. Technol.*, 47, 12819-12826, doi: 10.1021/es402687w, 2013a.
- 586 Lee, H. J., Laskin, A., Laskin, J., and Nizkorodov, S. A.: Excitation Emission Spectra and Fluorescence
 587 Quantum Yields for Fresh and Aged Biogenic Secondary Organic Aerosols, *Environ. Sci. Technol.*, 47,
 588 5763-5770, doi: 10.1021/es400644c, 2013b.
- 589 Lin, J.-L., Lin, Y.-C., Lin, B.-C., Lai, P.-C., Chien, T.-E., Li, S.-H., and Lin, Y.-F.: Adsorption and
 590 Reactions on TiO₂: Comparison of N,N-Dimethylformamide and Dimethylamine, *J. Phys. Chem. C*, 118,
 591 20291-20297, doi: 10.1021/jp5044859, 2014.
- 592 Liu, X., Zhang, Y., Han, W., Tang, A., Shen, J., Cui, Z., Vitousek, P., Erisman, J. W., Goulding, K.,
 593 Christie, P., Fangmeier, A., and Zhang, F.: Enhanced nitrogen deposition over China, *Nature*, 494, 459-
 594 462, doi:10.1038/nature11917, 2013.
- 595 Liu, Y., He, H., and Mu, Y.: Heterogeneous reactivity of carbonyl sulfide on α -Al₂O₃ and γ -Al₂O₃, *Atmos.*
 596 *Environ.*, 42, 960-969, doi: 10.1016/j.atmosenv.2007.10.007, 2008.
- 597 Liu, Y., He, H., and Ma, Q.: Temperature Dependence of the Heterogeneous Reaction of Carbonyl Sulfide
 598 on Magnesium Oxide, *J. Phys. Chem. A*, 112, 2820-2826, doi: 10.1021/jp711302r, 2008
- 599 Liu, Y., and He, H.: Experimental and Theoretical Study of Hydrogen Thiocarbonate for Heterogeneous
 600 Reaction of Carbonyl Sulfide on Magnesium Oxide, *J. Phys. Chem. A*, 113 3387-3394, doi:
 601 10.1021/jp809887c, 2009
- 602 Liu, Y., Ma, J., and He, H.: Heterogeneous reactions of carbonyl sulfide on mineral oxides: mechanism
 603 and kinetics study, *Atmos. Chem. Phys.*, 10, 10335-10344, doi: 10.5194/acp-10-10335-2010, 2010a.
- 604 Liu, Y., Ma, J., Liu, C., and He, H.: Heterogeneous uptake of carbonyl sulfide onto kaolinite within a
 605 temperature range of 220–330 K, *J. Geophys. Res.*, 115(D24311), doi:10.1029/2010JD014778, 2010b.
- 606 Liu, Y., Han, C., Liu, C., Ma, J., Ma, Q., and He, H.: Differences in the reactivity of ammonium salts
 607 with methylamine, *Atmos. Chem. Phys.*, 12, 4855-4865, doi: 10.5194/acp-12-4855-2012, 2012a.
- 608 Liu, Y., Ma, Q., and He, H.: Heterogeneous uptake of amines by citric acid and humid acid, *Environ. Sci*
 609 *Technol.*, 46, 11112-11118, doi: 10.1021/es302414v, 2012b.
- 610 Liu, Y., Han, C., Ma, J., Bao, X., and He, H.: Influence of relative humidity on heterogeneous kinetics of



- 611 NO₂ on kaolin and hematite, *Phys. Chem. Chem. Phys.*, 17, 19424-19431, doi: 10.1039/C5CP02223A,
612 2015a.
- 613 Liu, Y., Liggio, J., Staebler, R., and Li, S. M.: Reactive uptake of ammonia to secondary organic aerosols:
614 kinetics of organonitrogen formation, *Atmos. Chem. Phys.*, 15, 13569-13584, doi: 10.5194/acp-15-
615 13569-2015, 2015b.
- 616 Lloyd, J. A., Heaton, K. J., and Johnston, M. V.: Reactive Uptake of Trimethylamine into Ammonium
617 Nitrate Particles, *J. Phys. Chem. A*, 113, 4840-4843, doi: 10.1021/jp900634d, 2009.
- 618 Meunier, C. L., Gundale, M. J., Sanchez, I. S., and Liess, A.: Impact of nitrogen deposition on forest and
619 lake food webs in nitrogen-limited environments, *Glob. Change Biol.*, 22, 164-179, doi:
620 10.1111/gcb.12967, 2016.
- 621 Miranda-Trevino I, J. C., and Coles, C. A.: Kaolinite properties, structure and influence of metal retention
622 on pH, *Appl. Clay Sci.*, 23, 133-139, doi:10.1016/S0169-1317(03)00095-4, 2003.
- 623 Muñoz, M. S. S., and Rossi, M. J.: Heterogeneous reactions of HNO₃ with flame soot generated under
624 different combustion conditions. Reaction mechanism and kinetics, *Phys. Chem. Chem. Phys.*, 4, 5110-
625 5118, doi: 10.1039/b203912p, 2002.
- 626 Murphy, S. M., Sorooshian, A., Kroll, J. H., Ng, N. L., Chhabra, P., Tong, C., Surratt, J. D., Knipping, E.,
627 Flagan, R. C., and Seinfeld, J. H.: Secondary aerosol formation from atmospheric reactions of aliphatic
628 amines, *Atmos. Chem. Phys.*, 7, 2313-2337, doi:10.5194/acp-7-2313-2007, 2007.
- 629 Murphy, W. F., Zerbetto, F., Duncan, J. L., and McKean, D. C.: Vibrational spectrum and harmonic force
630 field of trimethylamine, *J. Phys. Chem.*, 97, 581-595, doi: 10.1021/j100105a010, 1993.
- 631 Ndour, M., D'Anna, B., George, C., Ka, O., Balkanski, Y., Kleffmann, J., Stemmler, K., and Ammann,
632 M.: Photoenhanced uptake of NO₂ on mineral dust: Laboratory experiments and model simulations,
633 *Geophys. Res. Lett.*, 35, L05812, doi: 10.1029/2007gl032006, 2008.
- 634 Nguyen, T. B., Laskin, A., Laskin, J., and Nizkorodov, S. A.: Brown carbon formation from
635 ketoaldehydes of biogenic monoterpenes, *Faraday Discuss.*, 165, 473-494, doi: 10.1039/C3FD00036B,
636 2013.
- 637 Nishino, N., Arquero, K. D., Dawson, M. L., and Finlayson-Pitts, B. J.: Infrared studies of the reaction
638 of methanesulfonic acid with trimethylamine on surfaces, *Environ. Sci. Technol.*, 48, 323-330, doi:
639 10.1021/es403845b, 2014.
- 640 Nunes, M. H. O., Silva, V. T. d., and Schmal, M.: The effect of copper loading on the acidity of
641 Cu/HZSM-5 catalysts: IR of ammonia and methanol for methylamines synthesis, *Appl. Catal. A: General*,
642 294, 148-155, doi: 10.1016/j.apcata.2005.06.031, 2005.
- 643 Ongwande, M., Morrison, G. C., Guo, X., and Chusuei, C. C.: Adsorption of trimethylamine on
644 zirconium silicate and polyethylene powder surfaces, *Colloid Surf. A: Physicochem. Eng. Asp.*, 310,
645 62-67, doi: 10.1016/j.colsurfa.2007.05.076, 2007.
- 646 Prinn, R. G., Huang, J., Weiss, R. F., Cunnold, D. M., Fraser, P. J., Simmonds, P. G., McCulloch, A.,
647 Harth, C., Salameh, P., O'Doherty, S., Wang, R. H. J., Porter, L., and Miller, B. R.: Evidence for
648 Substantial Variations of Atmospheric Hydroxyl Radicals in the Past Two Decades, *Science*, 292, 1882-
649 1888, doi: 10.1126/science.1058673, 2001.
- 650 Qiu, C., Wang, L., Lal, V., Khalizov, A. F., and Zhang, R.: Heterogeneous Reactions of Alkylamines with
651 Ammonium Sulfate and Ammonium Bisulfate, *Environ. Sci. Technol.*, 45, 4748-4755, doi:
652 10.1021/es1043112, 2011.
- 653 Qiu, C., and Zhang, R.: Physicochemical Properties of Alkylammonium Sulfates: Hygroscopicity,
654 Thermostability, and Density, *Environ. Sci. Technol.*, 46, 4474-4480, doi: 10.1021/es3004377, 2012.
- 655 Qiu, C., and Zhang, R.: Multiphase chemistry of atmospheric amines, *Phys. Chem. Chem. Phys.*, 15,
656 5738-5752, doi: 10.1039/c3cp43446j, 2013.
- 657 Salam, A., Lohmann, U., Crenna, B., Lesins, G., Klages, P., Rogers, D., Irani, R., MacGillivray, A., and
658 Coffin, M.: Ice Nucleation Studies of Mineral Dust Particles with a New Continuous Flow Diffusion
659 Chamber, *Aerosol Sci. Technol.*, 40, 134-143, doi: 10.1080/02786820500444853, 2006.
- 660 Seisel, S., Lian, Y., Keil, T., Trukhin, M. E., and Zellner, R.: Kinetics of the interaction of water vapour
661 with mineral dust and soot surfaces at T = 298 K, *Phys. Chem. Chem. Phys.*, 6, 1926-1932, doi:
662 10.1039/B314568A, 2004.
- 663 Seisel, S., Børnsen, C., Vogt, R., and Zellner, R.: Kinetics and mechanism of the uptake of N₂O₅ on
664 mineral dust at 298K, *Atmos. Chem. Phys.*, 5, 3423-3432, doi: 10.5194/acp-5-3423-2005, 2005.
- 665 Smith, I. W. M.: Laboratory Studies of Atmospheric Reactions at Low Temperatures, *Chem. Rev.*, 103,
666 4549-4564, doi: 10.1021/cr020512r, 2003.
- 667 Smith, J. N., Barsanti, K. C., Friedli, H. R., Ehn, M., Kulmala, M., Collins, D. R., H. Scheckman, J.,
668 Williams, B. J., and McMurry, P. H.: Observations of aminium salts in atmospheric nanoparticles and
669 possible climatic implications, *Proc. Natl. Acad. Sci. USA*, 107, 6634-6639, doi:
670 10.1073/pnas.0912127107, 2010.



- 671 Tang, M. J., Thieser, J., Schuster, G., and Crowley, J. N.: Uptake of NO_3 and N_2O_5 to Saharan dust,
672 ambient urban aerosol and soot: a relative rate study, *Atmos. Chem. Phys.*, 10, 2965-2974, doi:
673 10.5194/acp-10-2965-2010, 2010.
- 674 Trainic, M., Riziq, A. A., Lavi, A., Flores, J. M., and Rudich, Y.: The optical, physical and chemical
675 properties of the products of glyoxal uptake on ammonium sulfate seed aerosols, *Atmos. Chem. Phys.*,
676 11, 9697-9707, doi: 10.5194/acp-11-9697-2011, 2011.
- 677 Underwood, G. M., Li, P., Al-Abadleh, H. A., and Grassian, V. H.: A Knudsen cell study of the
678 heterogeneous reactivity of nitric acid on oxide and mineral dust particles, *J. Phys. Chem. A*, 105, 6609-
679 6620, doi: 10.1021/jp002223h, 2001.
- 680 Usher, C. R., Michel, A. E., and Grassian, V. H.: Reactions on Mineral Dust, *Chem. Rev.*, 103, 4883-
681 4939, doi: 10.1021/cr020657y, 2003.
- 682 van Breemen, N.: Nitrogen cycle: Natural organic tendency, *Nature*, 415, 381-382, doi: 10.1038/415381a,
683 2002.
- 684 Wang, L., Lal, V., Khalizov, A. F., and Zhang, R.: Heterogeneous Chemistry of Alkylamines with Sulfuric
685 Acid: Implications for Atmospheric Formation of Alkylammonium Sulfates, *Environ. Sci. Technol.*, 44
686 2461-2465, doi: 10.1021/es9036868, 2010a.
- 687 Wang, L., Wang, W., and Ge, M.: Heterogeneous uptake of NO_2 on soils under variable temperature and
688 relative humidity conditions, *J. Environ. Sci.*, 24, 1759-1766, doi: 10.1016/S1001-0742(11)61015-2,
689 2012.
- 690 Wang, X. F., Gao, S., Yang, X., Chen, H., Chen, J. M., Zhuang, G. S., Surratt, J. D., Chan, M. N., and
691 Seinfeld, J. H.: Evidence for High Molecular Weight Nitrogen-Containing Organic Salts in Urban
692 Aerosols, *Environ. Sci. Technol.*, 44, 4441-4446, doi: 10.1021/es1001117, 2010b.
- 693 Wex, H., DeMott, P. J., Tobo, Y., Hartmann, S., Rösch, M., Clauss, T., Tomsche, L., Niedermeier, D., and
694 Stratmann, F.: Kaolinite particles as ice nuclei: learning from the use of different kaolinite samples and
695 different coatings, *Atmos. Chem. Phys.*, 14, 5529-5546, doi: 10.5194/acp-14-5529-2014, 2014.
- 696 Yu, G., Bayer, A. R., Galloway, M. M., Korshavn, K. J., Fry, C. G., and Keutsch, F. N.: Glyoxal in
697 Aqueous Ammonium Sulfate Solutions: Products, Kinetics and Hydration Effects, *Environ. Sci. Technol.*,
698 45, 6336-6342, doi: 10.1021/es200989n, 2011.
- 699 Zarzana, K. J., De Haan, D. O., Freedman, M. A., Hasenkopf, C. A., and Tolbert, M. A.: Optical
700 Properties of the Products of α -Dicarbonyl and Amine Reactions in Simulated Cloud Droplets, *Environ.*
701 *Sci. Technol.*, 46, 4845-4851, doi: 10.1021/es2040152, 2012.
- 702 Zhang, H. F., Ren, S. Y., Yu, J. W., and Yang, M.: Occurrence of selected aliphatic amines in source water
703 of major cities in China, *J. Environ. Sci.*, 24, 1885-1890, doi: 10.1016/s1001-0742(11)61055-3, 2012.
- 704 Zhang, Y., and Carmichael, G. R.: The Role of Mineral Aerosol in Tropospheric Chemistry in East Asia—
705 A Model Study, *Journal of Applied Meteorology*, 38, 353-366, doi: 10.1175/1520-0450, 1999.
- 706 Zheng, B., Zhang, Q., Zhang, Y., He, K. B., Wang, K., Zheng, G. J., Duan, F. K., Ma, Y. L., and Kimoto,
707 T.: Heterogeneous chemistry: a mechanism missing in current models to explain secondary inorganic
708 aerosol formation during the January 2013 haze episode in North China, *Atmos. Chem. Phys.*, 15, 2031-
709 2049, doi: 10.5194/acp-15-2031-2015, 2015.
- 710
- 711

712 **Tables**713 Table 1. Comparison of the γ of amines on typical particles.

Amines	Particles	γ	T (K)	Ref.
MA	Kaolinite	$2.27 \pm 0.26 \times 10^{-3}$	300	This study
	Citric acid ^a	$7.31 \pm 1.13 \times 10^{-3}$	300	(Liu et al., 2012b)
	Humic acid ^a	$1.26 \pm 0.07 \times 10^{-5}$	300	(Liu et al., 2012b)
	(NH ₄) ₂ SO ₄ ^a	$6.30 \pm 1.03 \times 10^{-3}$	300	(Liu et al., 2012a)
	(NH ₄) ₂ SO ₄ ^b	$2.60\text{--}3.40 \times 10^{-2}$	293	(Qiu et al., 2011)
	NH ₄ HSO ₄ ^a	$1.78 \pm 0.36 \times 10^{-2}$	300	(Liu et al., 2012a)
	NH ₄ NO ₃ ^a	$8.79 \pm 1.99 \times 10^{-3}$	300	(Liu et al., 2012a)
	NH ₄ Cl ^a	$2.29 \pm 0.28 \times 10^{-3}$	300	(Liu et al., 2012a)
	62% H ₂ SO ₄ solution	$2.00 \pm 0.20 \times 10^{-2}$	283	(Wang et al., 2010a)
	71% H ₂ SO ₄ solution	$2.00 \pm 0.30 \times 10^{-2}$	283	(Wang et al., 2010a)
82% H ₂ SO ₄ solution	$3.00 \pm 0.50 \times 10^{-2}$	283	(Wang et al., 2010a)	
DMA	Kaolinite	$1.71 \pm 0.26 \times 10^{-3}$	300	This study
	Citric acid ^a	$6.65 \pm 0.49 \times 10^{-3}$	300	(Liu et al., 2012b)
	Humic acid ^a	$7.33 \pm 0.40 \times 10^{-6}$	300	(Liu et al., 2012b)
	(NH ₄) ₂ SO ₄ ^b	$3.20\text{--}3.40 \times 10^{-2}$	293	(Qiu et al., 2011)
	[(NH ₄) ₃ (SO ₄) ₂] ⁺ cluster ^c	0.85 ± 0.26	r.t.	(Bzdek et al., 2010b)
	[(NH ₄) ₂ (HSO ₄)] ⁺ cluster ^c	1.05 ± 0.26	r.t.	(Bzdek et al., 2010b)
	[(NH ₄) ₃ (HSO ₄) ₂] ⁺ cluster ^c	0.85 ± 0.22	r.t.	(Bzdek et al., 2010b)
	[(NH ₄) ₄ (HSO ₄) ₃] ⁺ cluster ^c	0.61 ± 0.15	r.t.	(Bzdek et al., 2010b)
	[(NH ₄) ₃ (NO ₃) ₂] ⁺ cluster ^c	0.53 ± 0.21	r.t.	(Bzdek et al., 2010b)
	30% (NH ₄) ₂ SO ₄ solution	$1.80\text{--}0.60 \times 10^{-2}$	293	(Qiu et al., 2011)
62% H ₂ SO ₄ solution	$3.00 \pm 0.60 \times 10^{-2}$	283	(Wang et al., 2010a)	
71% H ₂ SO ₄ solution	$2.50 \pm 0.40 \times 10^{-2}$	283	(Wang et al., 2010a)	
82% H ₂ SO ₄ solution	$3.20 \pm 0.30 \times 10^{-2}$	283	(Wang et al., 2010a)	
TMA	Kaolinite	$2.95 \pm 0.63 \times 10^{-3}$	300	This study
	Citric acid ^a	$5.82 \pm 0.68 \times 10^{-3}$	300	(Liu et al., 2012b)
	Humic acid ^a	$4.75 \pm 0.15 \times 10^{-6}$	300	(Liu et al., 2012b)
	(NH ₄) ₂ SO ₄ ^b	$2.40\text{--}2.90 \times 10^{-2}$	293	(Qiu et al., 2011)
	[(NH ₄) ₂ (HSO ₄)] ⁺ cluster ^c	0.90 ± 0.26	r.t.	(Bzdek et al., 2010b)
	[(NH ₄) ₃ (HSO ₄) ₂] ⁺ cluster ^c	0.66 ± 0.26	r.t.	(Bzdek et al., 2010b)
	[(NH ₄) ₄ (HSO ₄) ₃] ⁺ cluster ^c	0.64 ± 0.26	r.t.	(Bzdek et al., 2010b)
	[(NH ₄) ₃ (NO ₃) ₂] ⁺ cluster ^c	0.40 ± 0.12	r.t.	(Bzdek et al., 2010b)
	NH ₄ NO ₃ ^d	$2.00 \pm 2.00 \times 10^{-3}$	r.t.	(Lloyd et al., 2009)
	62% H ₂ SO ₄ solution	$2.20 \pm 0.20 \times 10^{-2}$	283	(Wang et al., 2010a)
71% H ₂ SO ₄ solution	$2.70 \pm 0.80 \times 10^{-2}$	283	(Wang et al., 2010a)	
82% H ₂ SO ₄ solution	$3.50 \pm 0.20 \times 10^{-2}$	283	(Wang et al., 2010a)	

714 Note: Note: ^a coarse particles (grounded crystalline); ^b coarse particles (crystalline or
 715 amorphous from solution); ^c 1-2 nm particles; ^d 20-500 nm particles

716

717 Table 2. The γ_{eff} of amines on kaolinite in the temperature range 232-300 K

Temperature (K)	γ_{eff} (MA)	γ_{eff} (DMA)	γ_{eff} (TMA)
232	$5.79 \pm 0.64 \times 10^{-3}$	$6.04 \pm 1.24 \times 10^{-3}$	$9.24 \pm 0.26 \times 10^{-3}$
237	$4.70 \pm 0.58 \times 10^{-3}$	-	-
248	$3.90 \pm 0.86 \times 10^{-3}$	$5.35 \pm 1.03 \times 10^{-3}$	$5.90 \pm 0.93 \times 10^{-3}$
258	-	-	$4.40 \pm 0.03 \times 10^{-3}$
263	$3.51 \pm 0.39 \times 10^{-3}$	$4.68 \pm 1.23 \times 10^{-3}$	-
278	$2.63 \pm 0.30 \times 10^{-3}$	$2.25 \pm 0.46 \times 10^{-3}$	$3.44 \pm 0.40 \times 10^{-3}$
300	$2.27 \pm 0.26 \times 10^{-3}$	$1.71 \pm 0.26 \times 10^{-3}$	$2.95 \pm 0.63 \times 10^{-3}$

718



719 **Figure captions**

720 **Figure 1.** Uptake curves and the corresponding uptake coefficient of amines on
721 kaolinite at 300 K. The sample mass was 19.3, 20.6 and 20.2 mg, respectively.

722 **Figure 2.** *In situ* FTIR spectra of amines adsorbed on kaolinite for 30 min at 300 K.
723 The IR spectra were recorded taking the dried kaolinite as reference.

724 **Figure 3.** Mass dependence of γ_{obs} for amines on kaolinite at 300 K. Error bars indicate
725 1σ for repeated experiments.

726 **Figure 4.** (A) Box chart for the γ_{eff} of amines on kaolinite measured at 300 K. (B)
727 Relationship between the γ_{eff} and the basicity of amines.

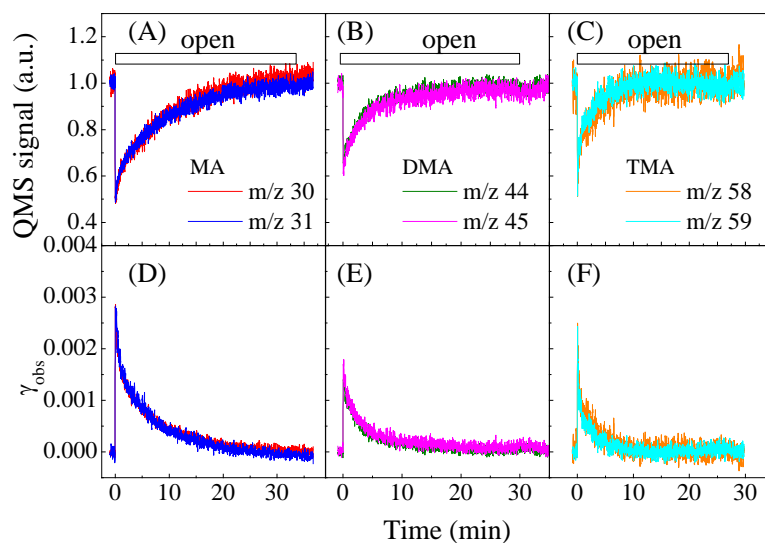
728 **Figure 5.** Temperature dependence of γ_{eff} for amines on kaolinite.

729

730

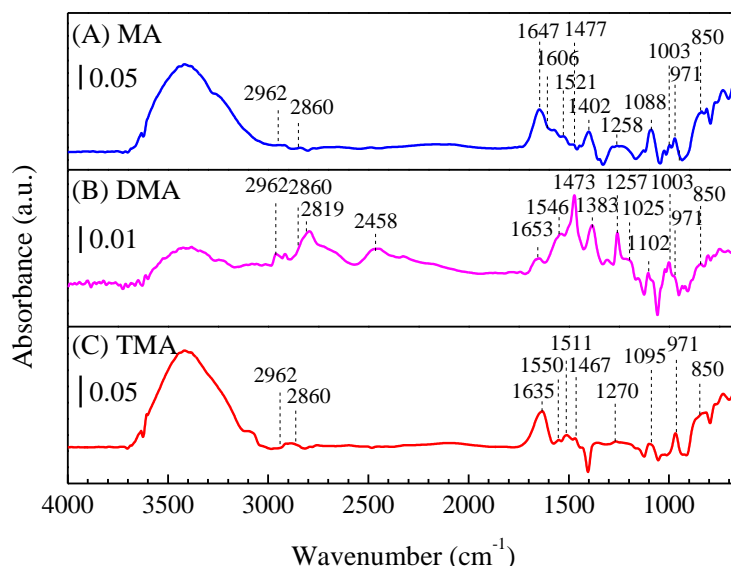


731 **Figures**



732
733

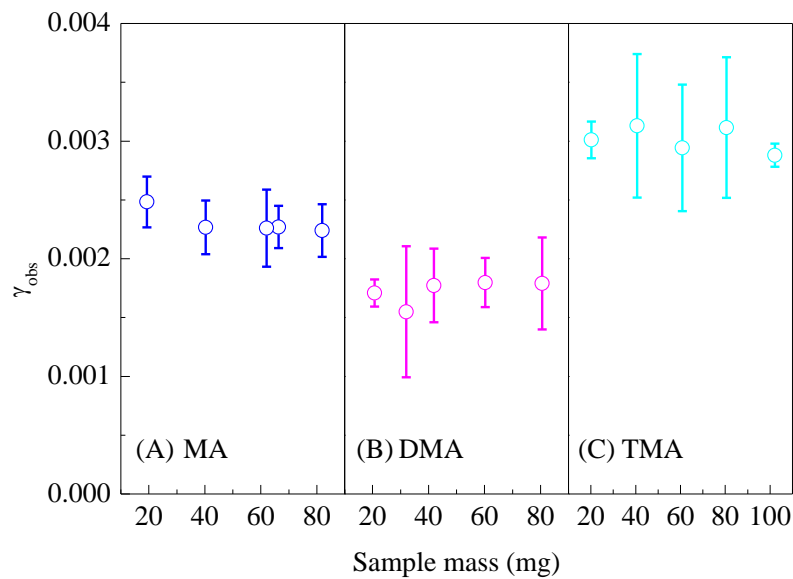
Fig. 1



734

735

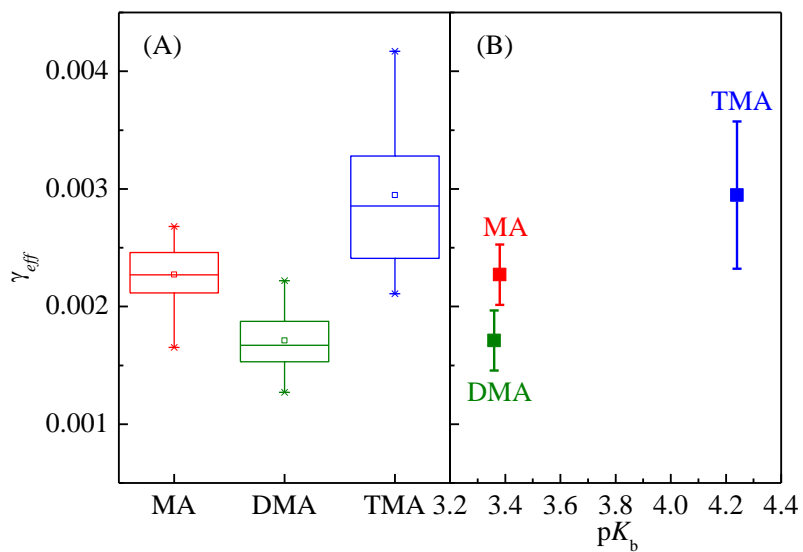
Fig. 2



736

737

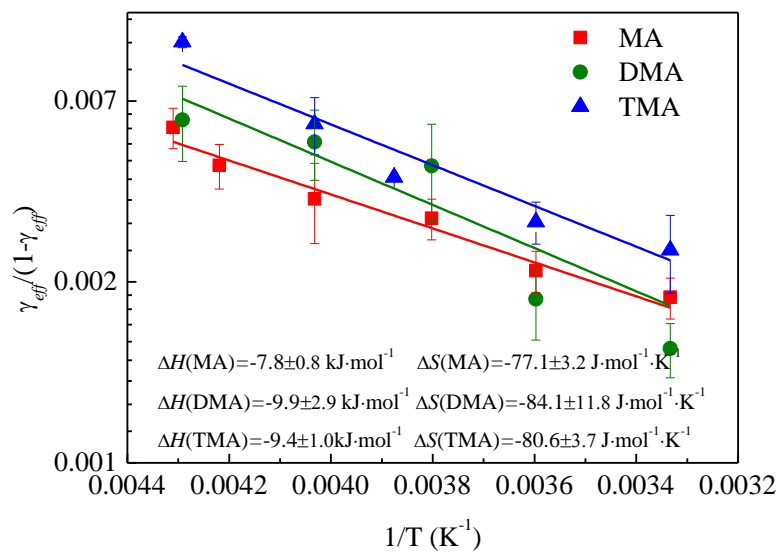
Fig. 3



738

739

Fig. 4



740

741

Fig. 5